



## Charged-current interactions of Kaon-decay-at-rest neutrinos

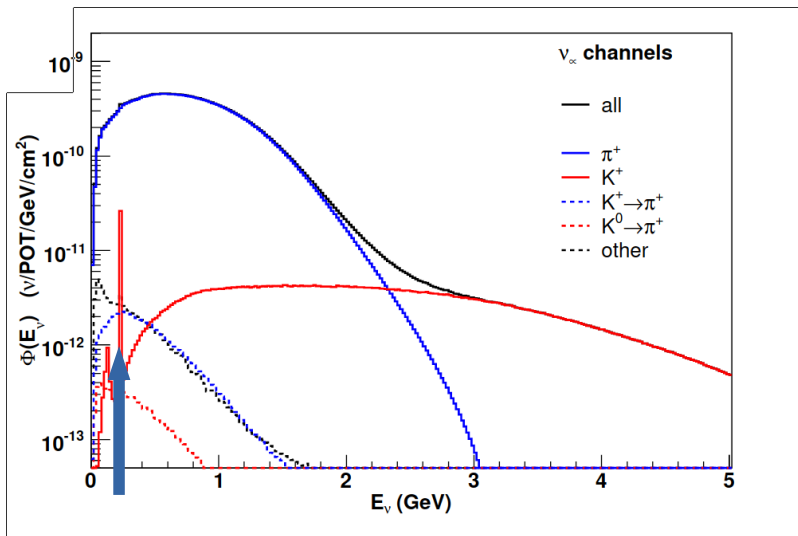
Alexis Nikolakopoulos

Based on work with N. Jachowicz, V. Pandey & J. Spitz

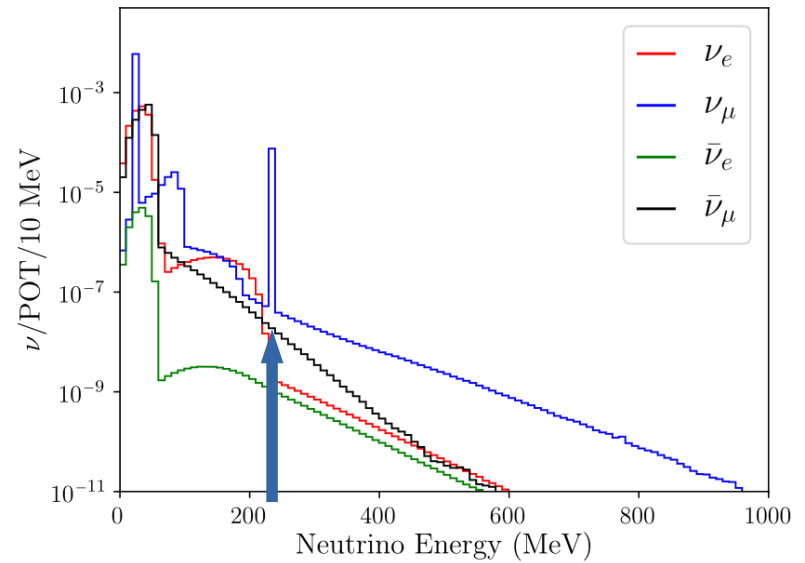
Interplay of Nuclear, Neutrino and BSM Physics at Low-Energies  
INT, University of Washington, 20 April 2023

# Muon neutrinos from stopped Kaon's in the absorber

## MiniBooNE



## JSNS<sup>2</sup>



KDAR produces  $\nu_\mu$  with  $E_\nu = 236 \text{ MeV}$

## What I will talk about

Opportunity of study of the nuclear response with monoenergetic  $\nu_\mu$

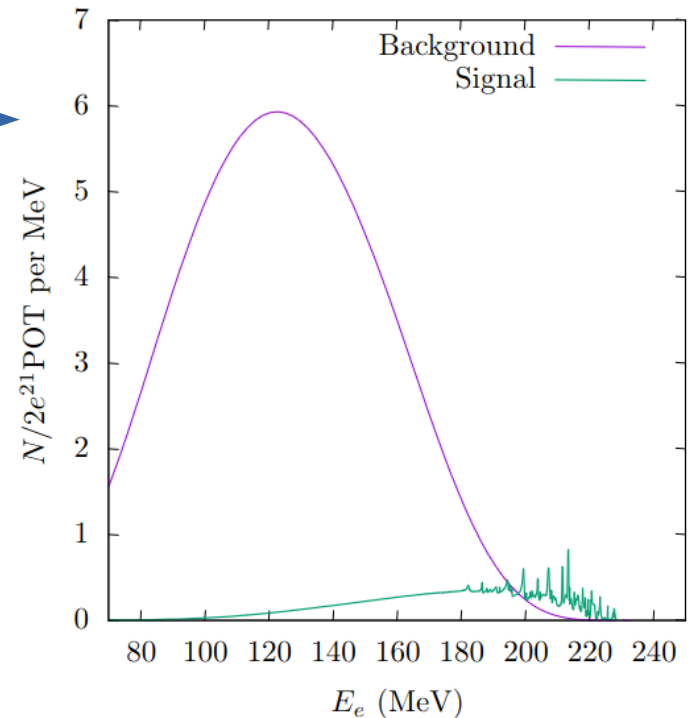
1. Angular dependence of electroweak nuclear response
2. Complementary electron scattering data
3. Measurements of KDAR  $\nu_\mu$  cross sections

## What I will NOT talk about

KDAR  $\nu_\mu$  oscillations on short-baselines to study MB excess

[J Spitz, PRD 85 093020]

Electron appearance in  $\nu_\mu$  from KDAR  
Background from  $\nu_e$  decays  
In LarTPC



[Phys. Rev. C 103, 064603 (2021)]

## What I will NOT talk about

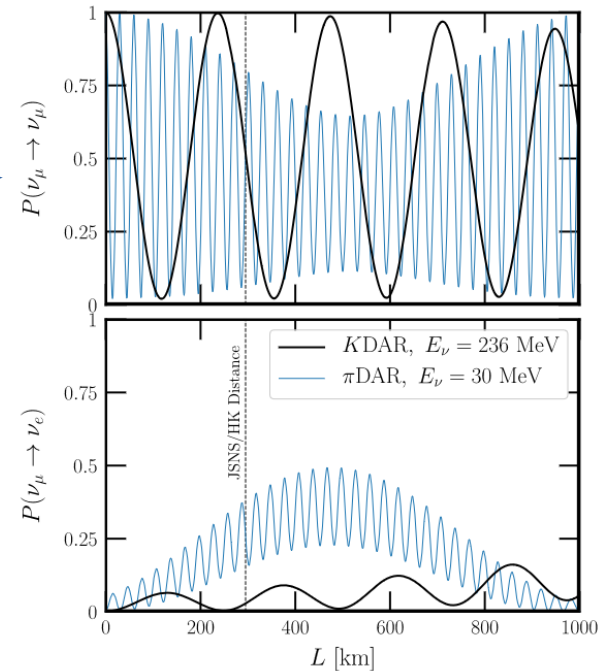
KDAR  $\nu_\mu$  oscillations on short-baselines to study MB excess

[J Spitz, PRD 85 093020]

Long-baseline  $\nu_\mu \rightarrow \nu_e$  oscillations with KDAR  $\nu_\mu$  from J-PARC MLF in HyperK

[R. Harnik, K.J. Kelly, P. Machado, PRD 101, 033008 (2020) ]

'standard' 3v oscillations at  
a fixed E/L



## What I will NOT talk about

KDAR  $\nu_\mu$  oscillations on short-baselines to study MB excess

[J Spitz, PRD 85 093020]

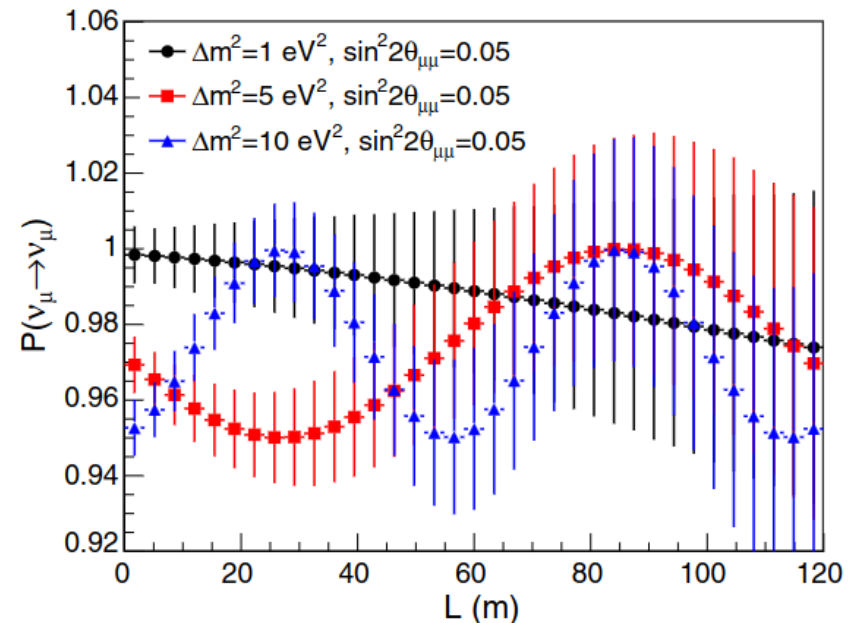
Long-baseline  $\nu_\mu \rightarrow \nu_e$  oscillations with KDAR  $\nu_\mu$  from J-PARC MLF in HyperK

[R. Harnik, K.J. Kelly, P. Machado, PRD 101, 033008 (2020) ]

“Kpipe”: A proposed 120 m long detector  
at JPARC MLF to search

For  $\nu_\mu$  disappearance at short-baseline

[S. Axani, G. Collin, J. M. Conrad, M. H. Shaevitz,  
J. Spitz, and T. Wongjirad PRD 92, 092010 ]



## Some generalities

$$\frac{d\sigma_X}{dE_f d\cos\theta_f} = \frac{F_X^2 E_f k_f}{2\pi} \times \\ [(V_{CC}R_{CC} + V_{CL}R_{CL} + V_{LL}R_{LL}) \\ + (V_T R_T + hV_{T'} R_{T'})].$$

$$J^\mu(q) = \int d\vec{r} e^{-i\vec{q}\cdot\vec{r}} \mathcal{J}^\mu(\mathbf{r}),$$

$$\mathcal{M}_{JM} = \int d\vec{r} [j_J(qr) Y_{JM}(\Omega_r)] \mathcal{J}^0(\vec{r})$$

$$\mathcal{L}_{JM} = \frac{i}{q} \int d\vec{r} \left[ \vec{\nabla} (j_J(qr) Y_{JM}(\Omega_r)) \right] \cdot \vec{\mathcal{J}}(\vec{r})$$

$$\mathcal{T}_{JM}^{el} = \frac{1}{q} \int d\vec{r} \left[ \vec{\nabla} \times j_J(qr) \vec{\mathcal{Y}}_{J(J,1)}^M(\Omega_r) \right] \cdot \vec{\mathcal{J}}(\vec{r})$$

$$\mathcal{T}_{JM}^{mag} = \int d\vec{r} \left[ j_J(qr) \vec{\mathcal{Y}}_{J(J,1)}^M(\Omega_r) \right] \cdot \vec{\mathcal{J}}(\vec{r}).$$

For 1-boson exchange  
(No coulomb, radiation)

Separation in lepton factors  
 $V(E, E', \cos\theta, m_l)$

And nuclear responses  
 $R(\omega, q)$

$$\omega = E - E', \quad q = |\mathbf{k} - \mathbf{k}'|$$

## Some generalities

$$\frac{d\sigma_X}{dE_f d\cos\theta_f} = \frac{F_X^2 E_f k_f}{2\pi} \times \\ [(V_{CC}R_{CC} + V_{CL}R_{CL} + V_{LL}R_{LL}) \\ + (V_T R_T + hV_{T'} R_{T'})].$$

$$R_{CC} = \sum_{J \geq 0} \sum_{J_f, J_i} |\langle J_f \| \mathcal{M}_J \| J_i \rangle|^2,$$

$$R_{LL} = \sum_{J \geq 0} \sum_{J_f, J_i} |\langle J_f \| \mathcal{L}_J \| J_i \rangle|^2,$$

$$R_{CL} = \sum_{J \geq 0} \sum_{J_f, J_i} 2\text{Re} [\langle J_f \| \mathcal{M}_J \| J_i \rangle \langle J_f \| \mathcal{L}_J \| J_i \rangle^*],$$

$$R_T = \sum_{J \geq 1} \sum_{J_f, J_i} |\langle J_f \| \mathcal{T}_J^{el} \| J_i \rangle|^2 + |\langle J_f \| \mathcal{T}_J^{mag} \| J_i \rangle|^2,$$

$$R_{T'} = \sum_{J \geq 1} \sum_{J_f, J_i} 2\text{Re} [\langle J_f \| \mathcal{T}_J^{el} \| J_i \rangle \langle J_f \| \mathcal{T}_J^{mag} \| J_i \rangle^*], \longrightarrow$$

For 1-boson exchange  
(No coulomb)

Separation in lepton factors  
 $V(E, E', \cos\theta, m_l)$

And nuclear responses  
 $R(\omega, q)$

$$\omega = E - E', \quad q = |\mathbf{k} - \mathbf{k}'|$$

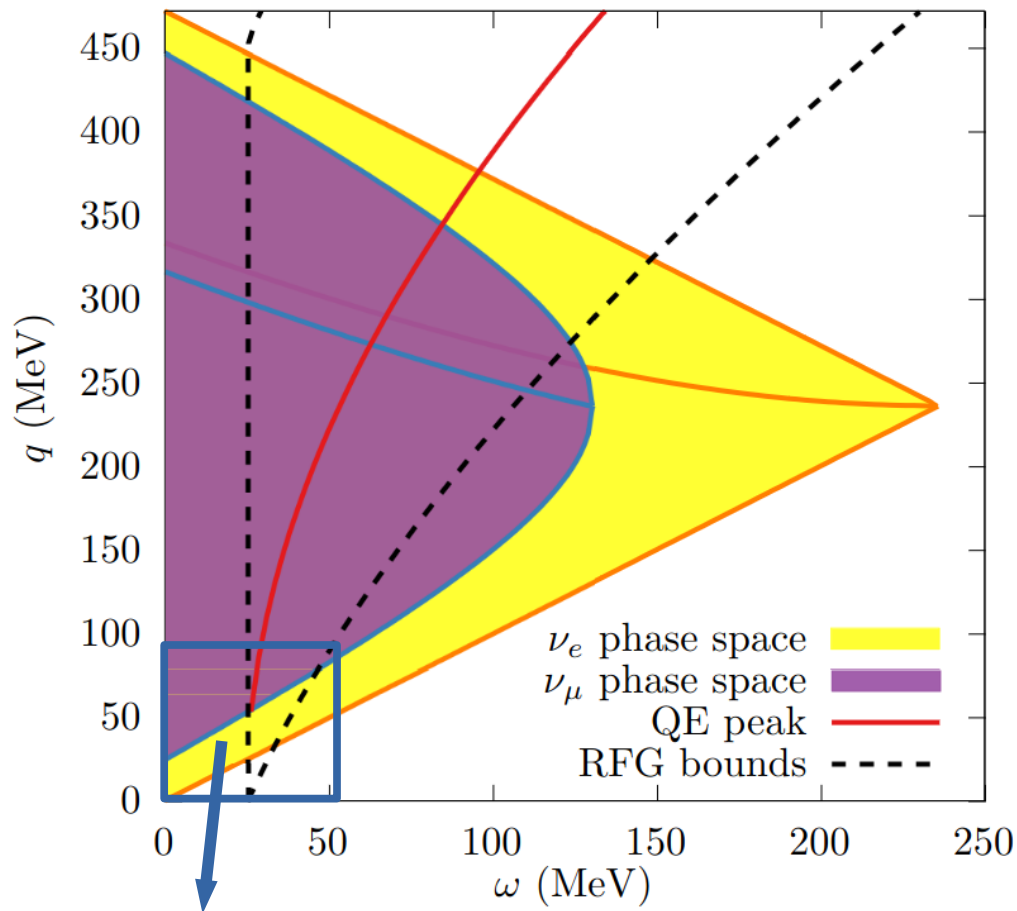
$$R_X = R_X^{AA} + R_X^{VV}$$

$$R_{X'} = R_{X'}^{VA}$$

Pure VA-  
interference



## KDAR phase space in energy- momentum transfer: Charged-current



KDAR  $\nu_\mu$  live in a 'transition region' between 'QE' scattering and low-energy excitations

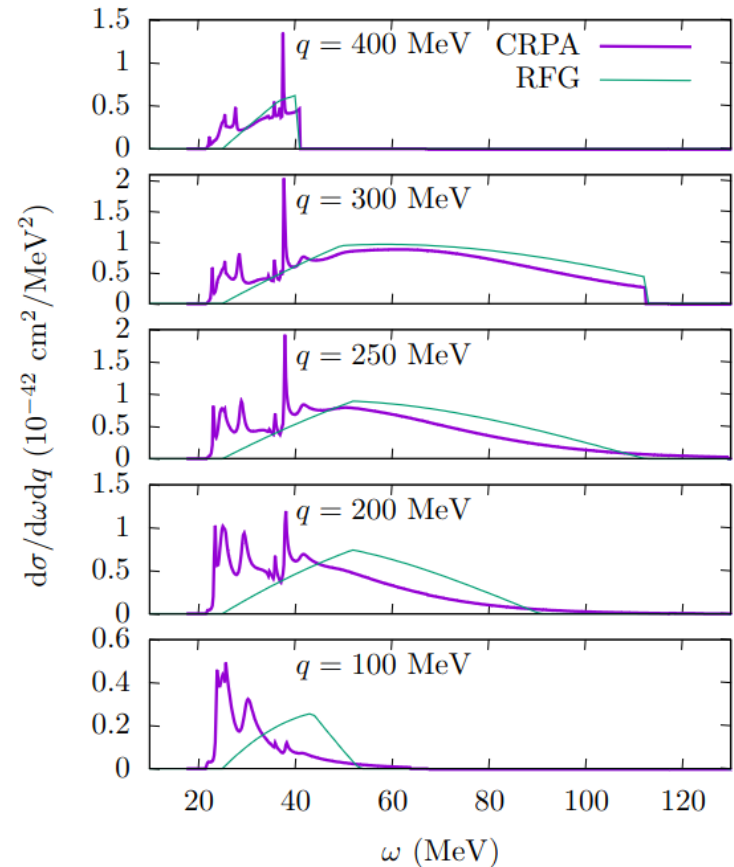
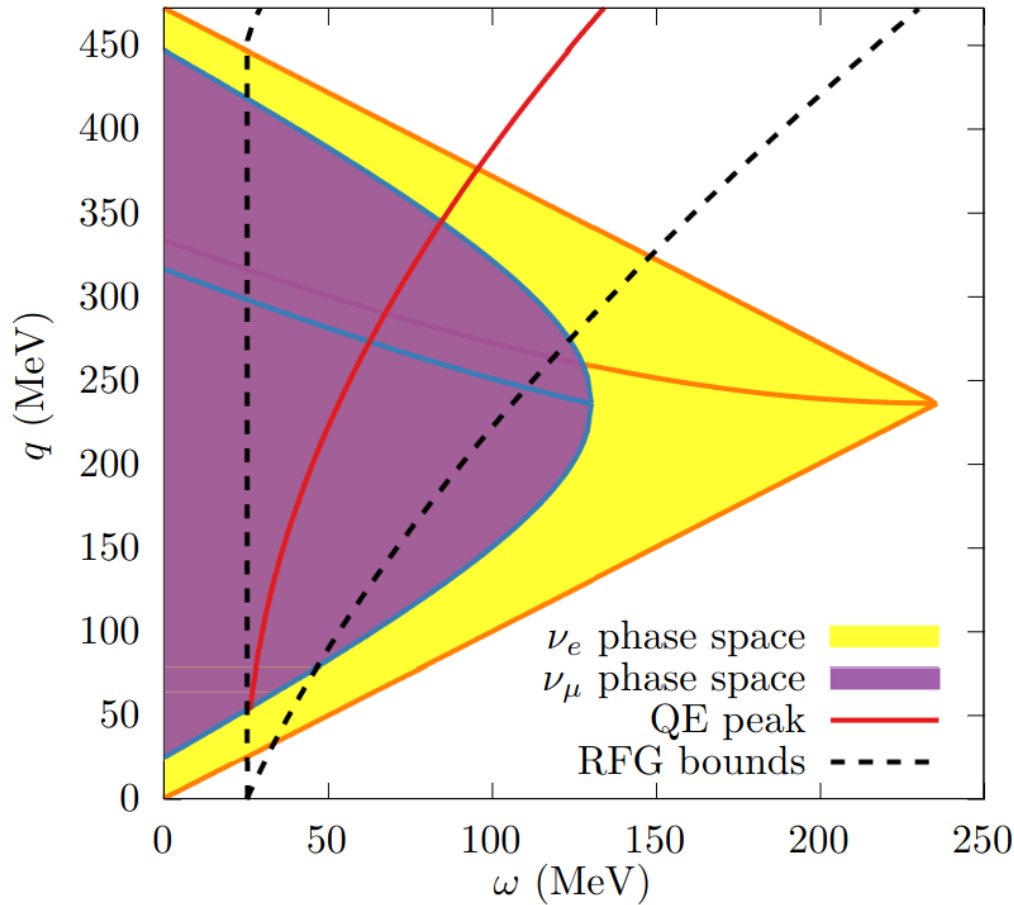
Monoenergetic **CC** scattering  
→ muon as a clear observable

Can use the muon angle to probe momentum transfer

Phase space for  $\pi$ DAR  $\nu_e$

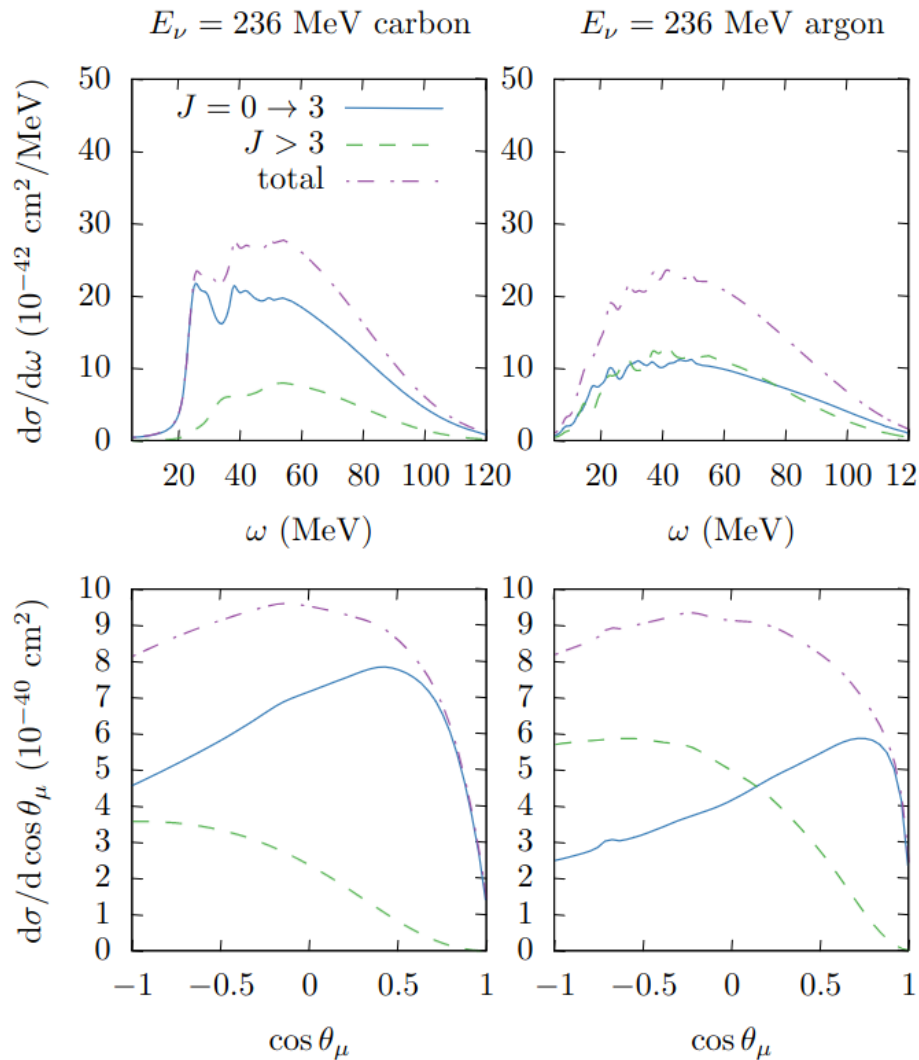
# KDAR phase space in energy- momentum transfer: Charged-current

'Transition region'

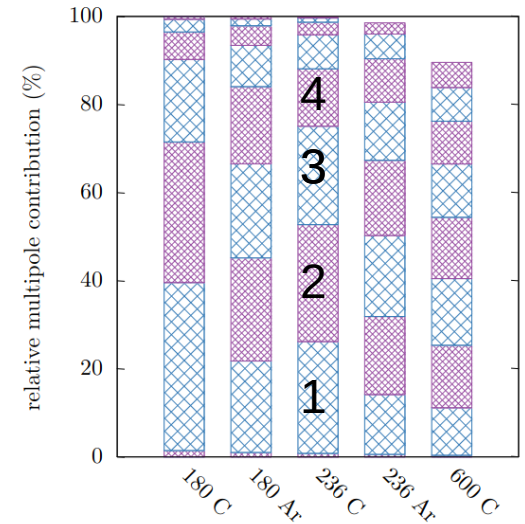


Momentum transfer  $q \leftrightarrow \cos\theta_{\mu^-}$  Inclusive measurements with angular resolution?

# Angular dependence of multipole contributions



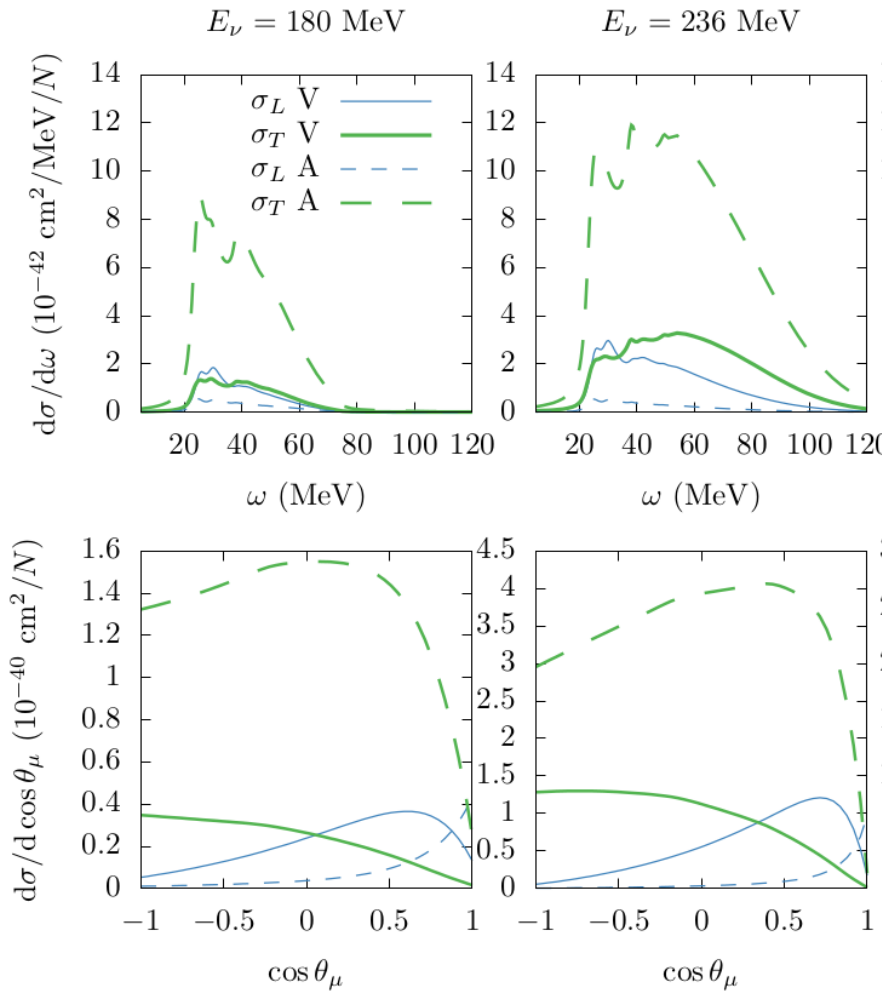
## Multipole contributions



Carbon CS  $\sim 6$  MPs  
 Argon CS  $\sim 9$  MPs

Carbon: separate low- $w$  structure  
 From  $\sim 3$  MP at forward angles

# Vector and Axial-vector contributions

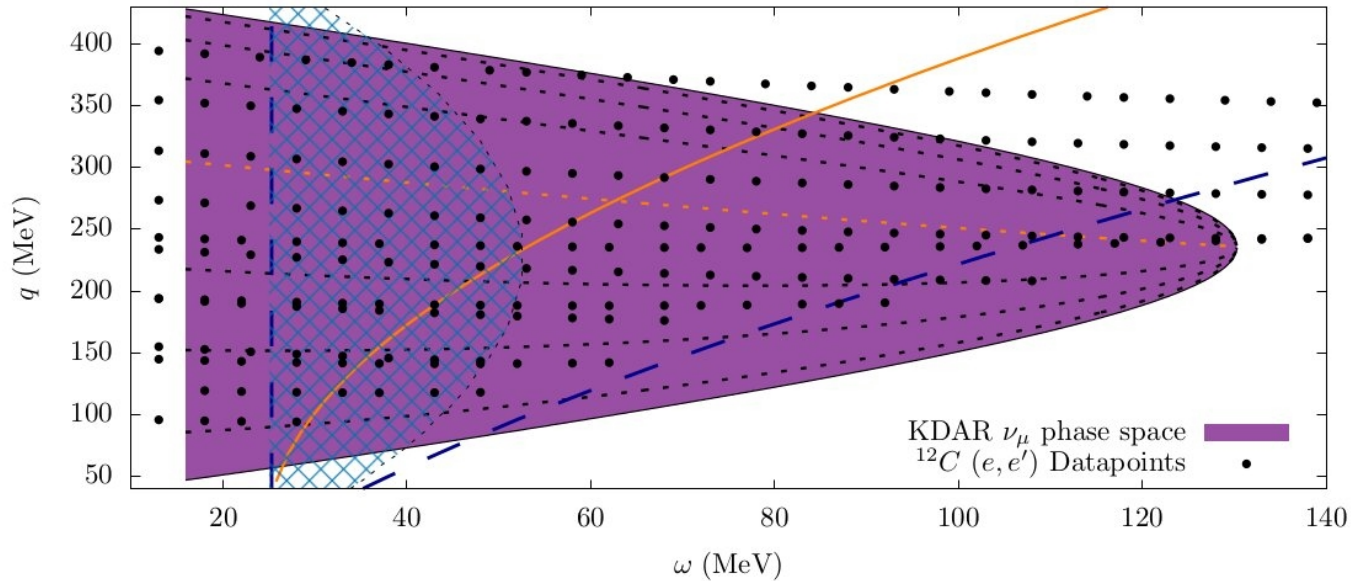


$$\begin{aligned}
 V_{CC} &= 1 + \frac{k_l}{E_l} \cos \theta_l, \\
 V_{CL} &= - \left( \frac{\omega}{q} V_{CC} + \frac{m_l^2}{E_l q} \right), \\
 V_{LL} &= V_{CC} - \frac{2E_i E_l}{q^2} \left( \frac{k_l}{E_l} \right)^2 \sin^2 \theta_l, \\
 V_T &= 2 - V_{CC} + \frac{E_i E_l}{q^2} \left( \frac{k_l}{E_l} \right)^2 \sin^2 \theta_l, \\
 V_{T'} &= \frac{E_i + E_l}{q} (2 - V_{CC}) - \frac{m_l^2}{E_f q}.
 \end{aligned}$$

$$\begin{aligned}
 \frac{d\sigma_X}{dE_f d \cos \theta_f} &= \frac{F_X^2 E_f k_f}{2\pi} \times \\
 \sigma_L &\leftarrow [(V_{CC} R_{CC} + V_{CL} R_{CL} + V_{LL} R_{LL}) \\
 &\quad + (V_T R_T + h V_{T'} R_{T'})]. \\
 &\quad \downarrow \\
 &\sigma_T
 \end{aligned}$$

Forward-backward separation L T

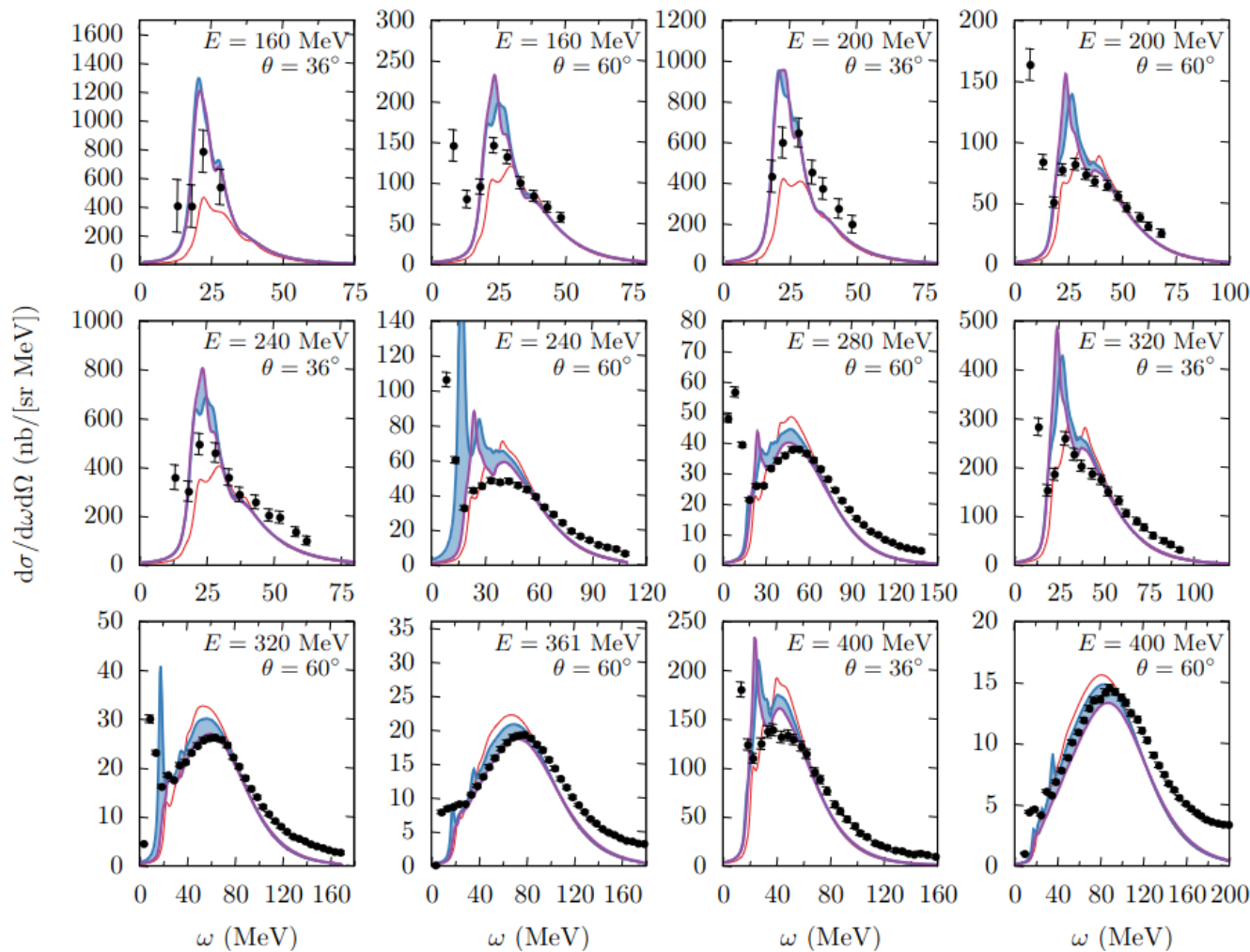
## Electron scattering in KDAR phase-space



Available phase space almost fully covered by  $(e, e')$  scattering on  $^{12}\text{C}$   
→ Can probe nuclear phase space with both  $e$  and  $\nu$ !

+New  $^{40}\text{Ar}$  data from Mainz ( $E=240$ ,  $\theta=20^\circ$ ), see talk J. Sobczyk

# Electron scattering in KDAR phase-space: $^{12}\text{C}$ HF-CRPA calculations (N. Jachowicz talk)



Sk-HF  
CRPA w cut-off  
CRPA

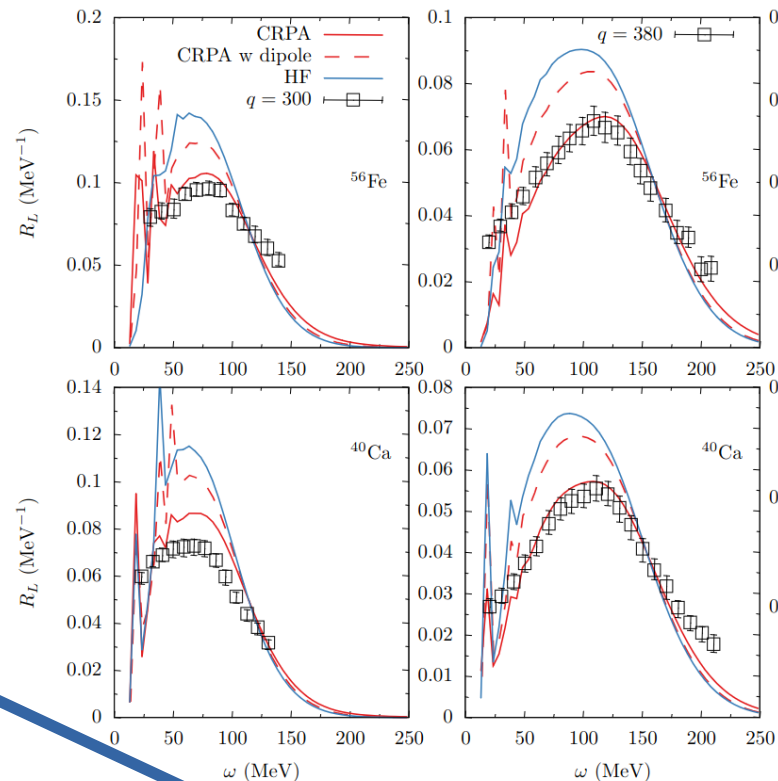
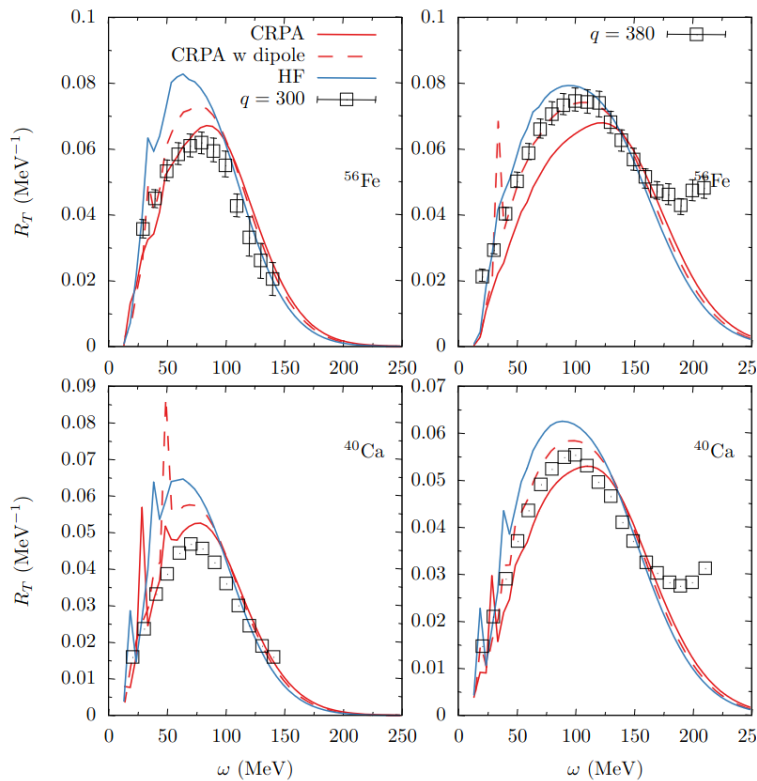
Cut-off FF in residual interaction  
Included

Low-q : prefer no FF  
High-q : FF needed

# Electron scattering in KDAR phase-space: Heavier targets

$R_T$

$R_L$



Fe

Ca

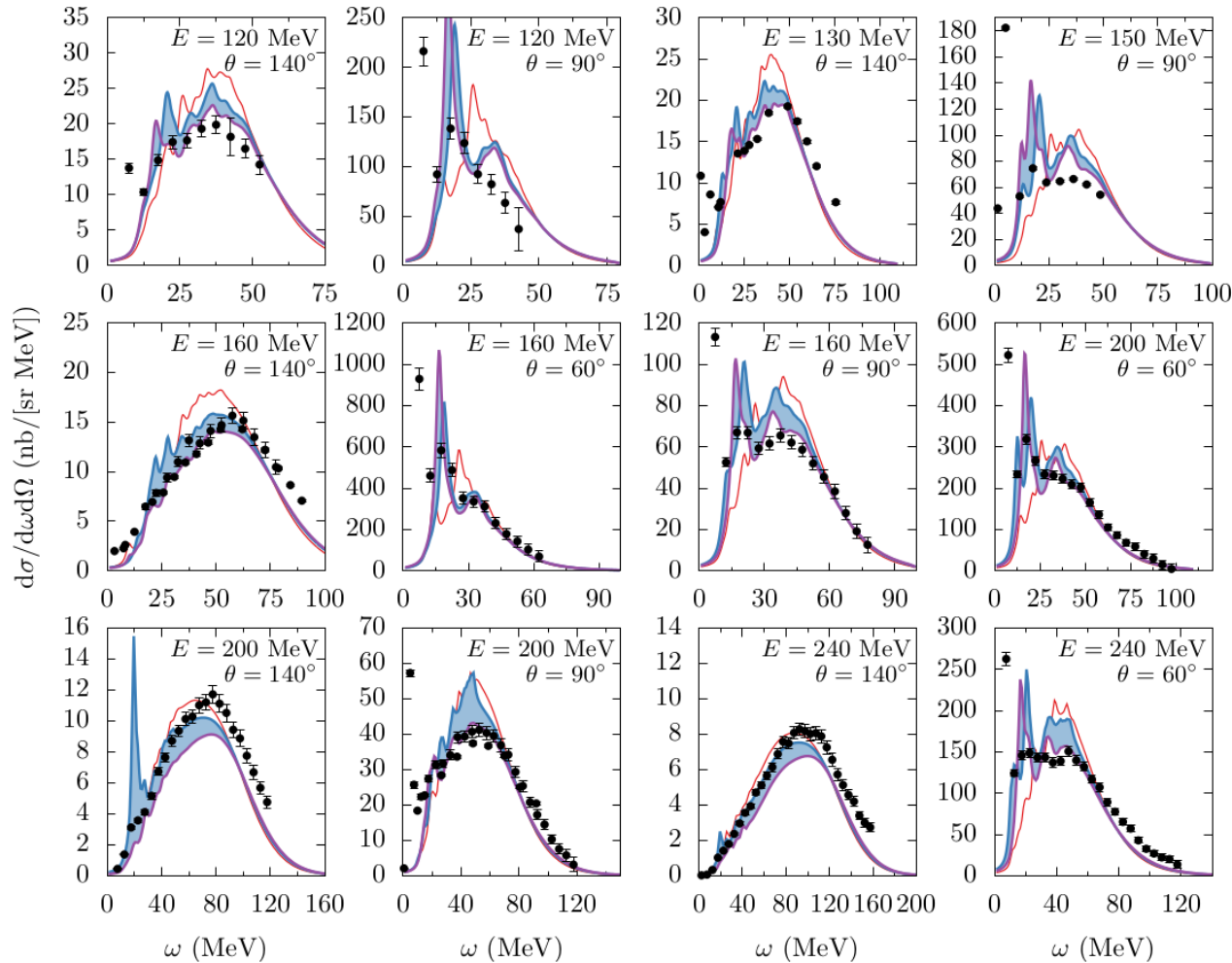
Low-q: no FF, high-q : FF needed ?

$R_T$  behaviour

$$\frac{d\sigma}{d\omega d\Omega} = \sigma_{\text{Mott}} \left[ \frac{Q^4}{q^4} R_L + \left( \frac{Q^2}{2q^2} + \tan^2 \frac{\theta_l}{2} \right) R_T \right]$$

# Electron scattering in KDAR phase-space: $^{40}\text{Ca}$

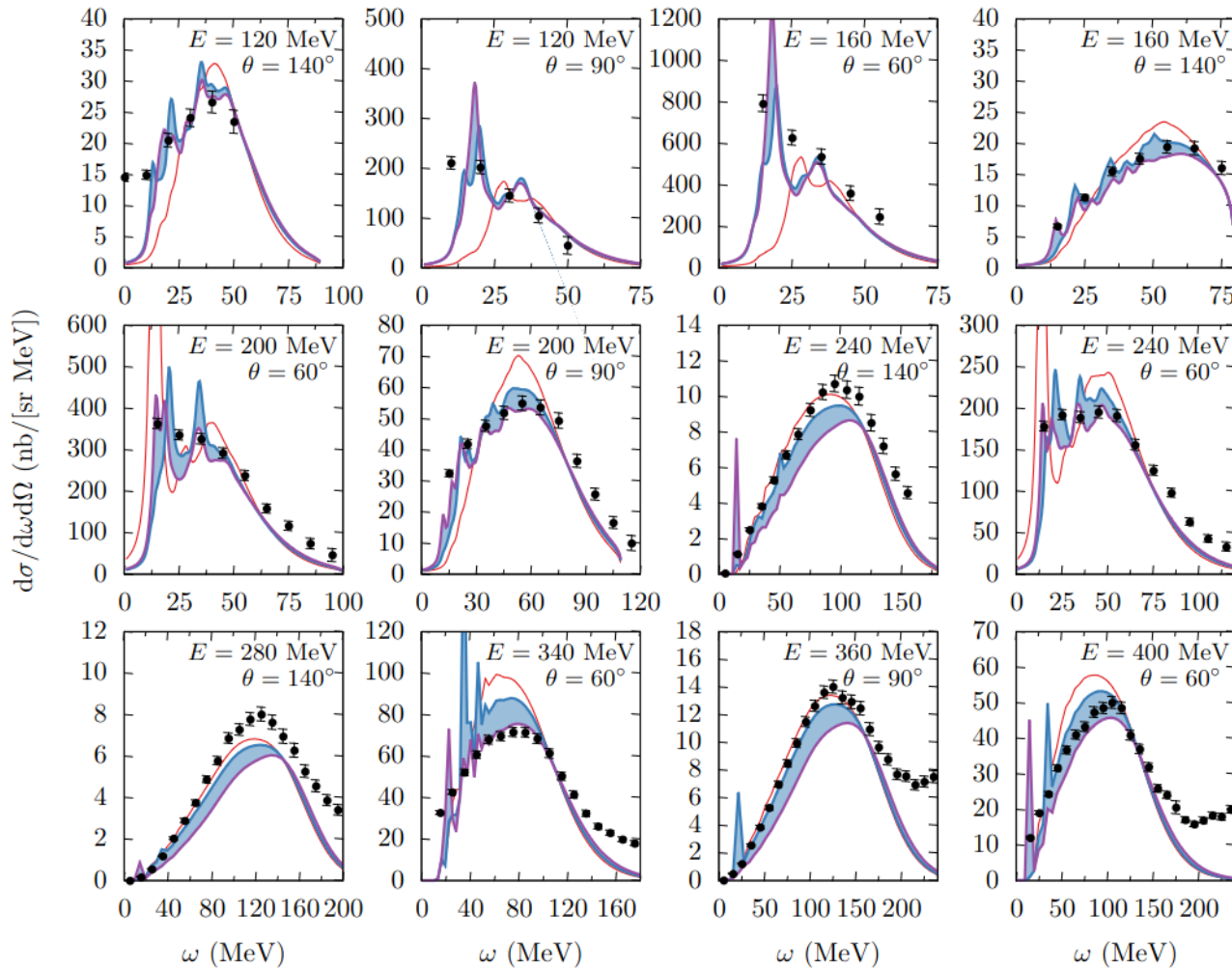
More detailed information from directly comparing to the cross section



Sk-HF  
CRPA w cut-off  
CRPA



# Electron scattering in KDAR phase-space: $^{56}\text{Fe}$



Sk-HF  
CRPA w cut-off  
CRPA

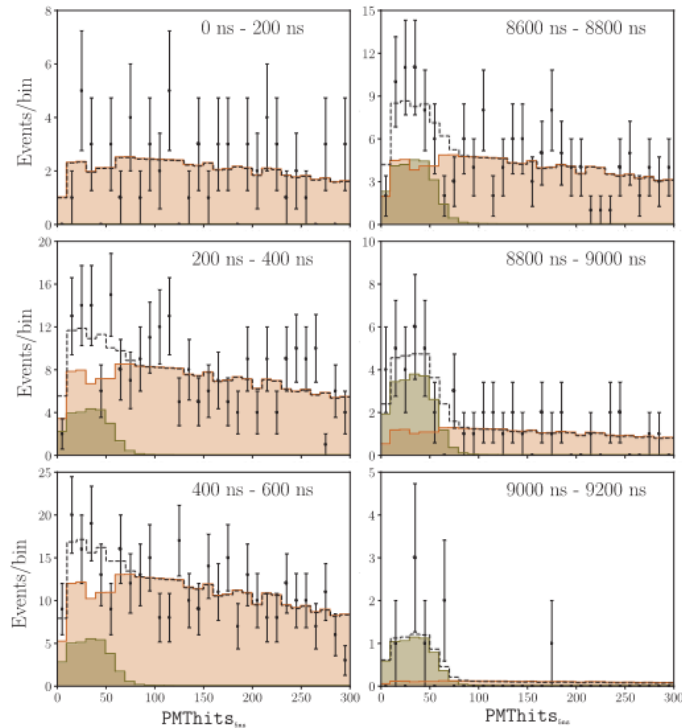
Robust results for  
 $^{12}\text{C}$ ,  $^{40}\text{Ca}$ ,  $^{56}\text{Fe}$

# Measurements of KDAR muon neutrino interactions

## MiniBooNE

PRL 120, 141802 (2018)

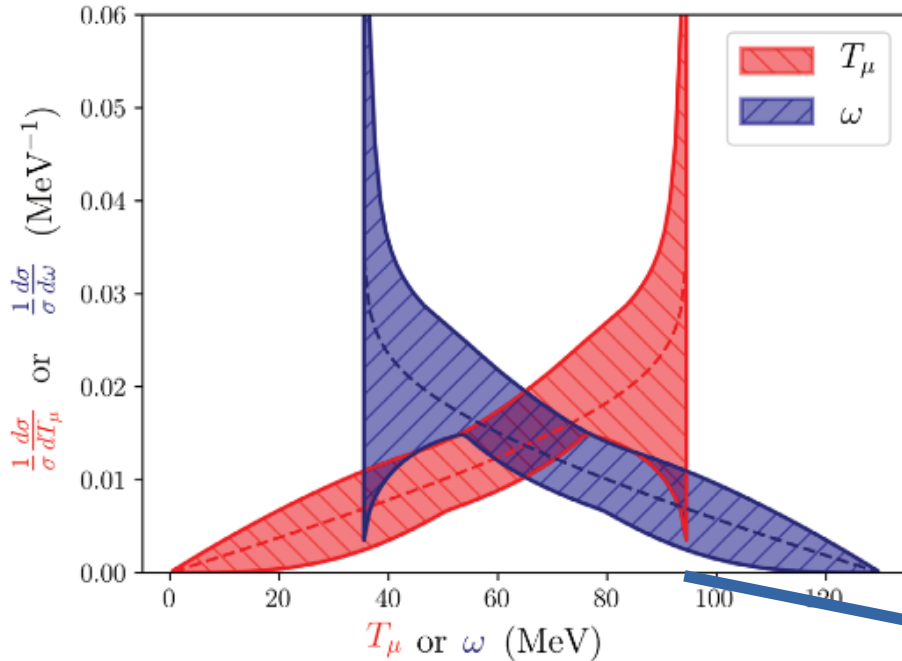
Isolate KDAR  $\nu_\mu$  from NuMI absorber



Timing info to separate from in-flight

# MiniBooNE shape measurement

PRL 120, 141802 (2018)



MiniBooNE performs a 'template-based' analysis

$$x^{a-1}(1-x)^{b-1} \frac{\Gamma(a+b)}{\Gamma(a)\Gamma(b)}, \quad x = \frac{T_\mu}{T_\mu^{max}}$$

Testing the consistency of the parametrized spectrum shape with the signal

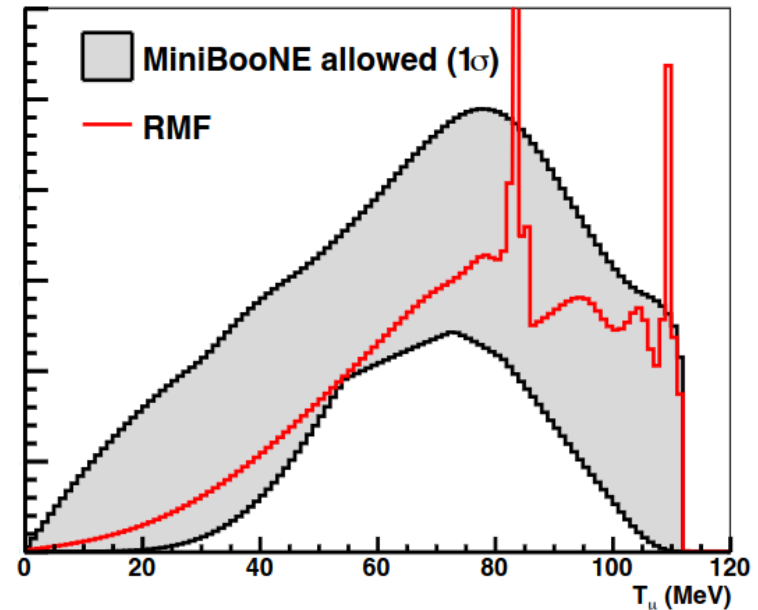
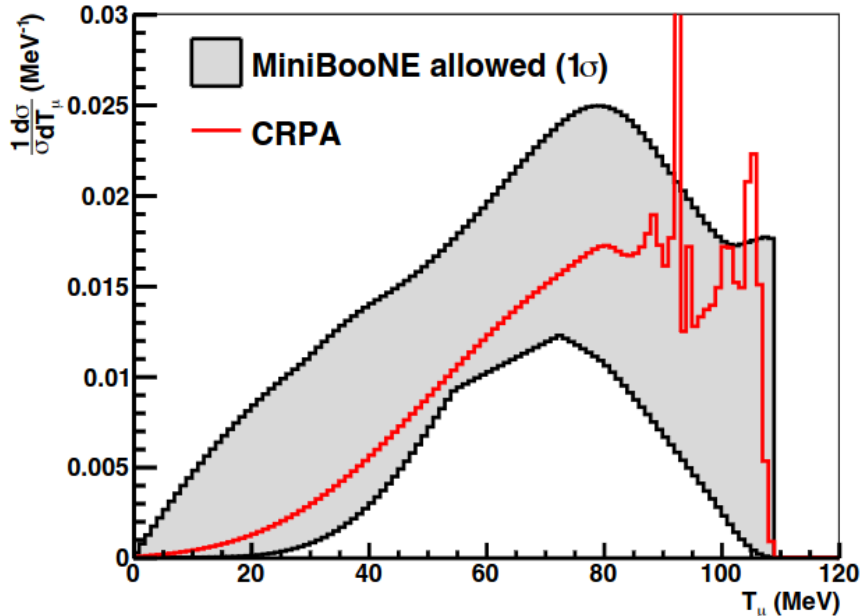
Depends on parameter  $T_\mu^{max}$   
 MB prefers  $T_\mu^{max} = 95 \text{ MeV}$

In principle  $T_\mu^{max} = E_\nu - m_\mu \approx 130 \text{ MeV}$

# MiniBooNE shape measurement

PRL 120, 141802 (2018)

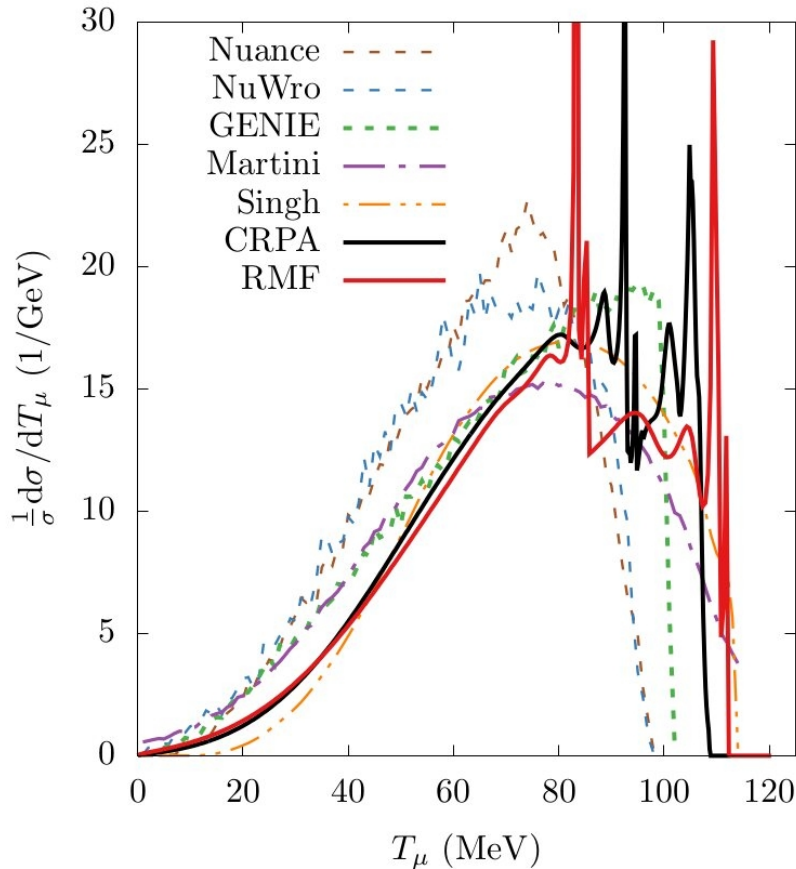
$$x^{a-1}(1-x)^{b-1} \frac{\Gamma(a+b)}{\Gamma(a)\Gamma(b)}, \quad x = \frac{T_\mu}{T_\mu^{max}}$$



Comparison to MB best fit template as function of endpoint (online tool)

Note: Best fit shape changes with the 'endpoint'

# MiniBooNE comparison: Model comparisons

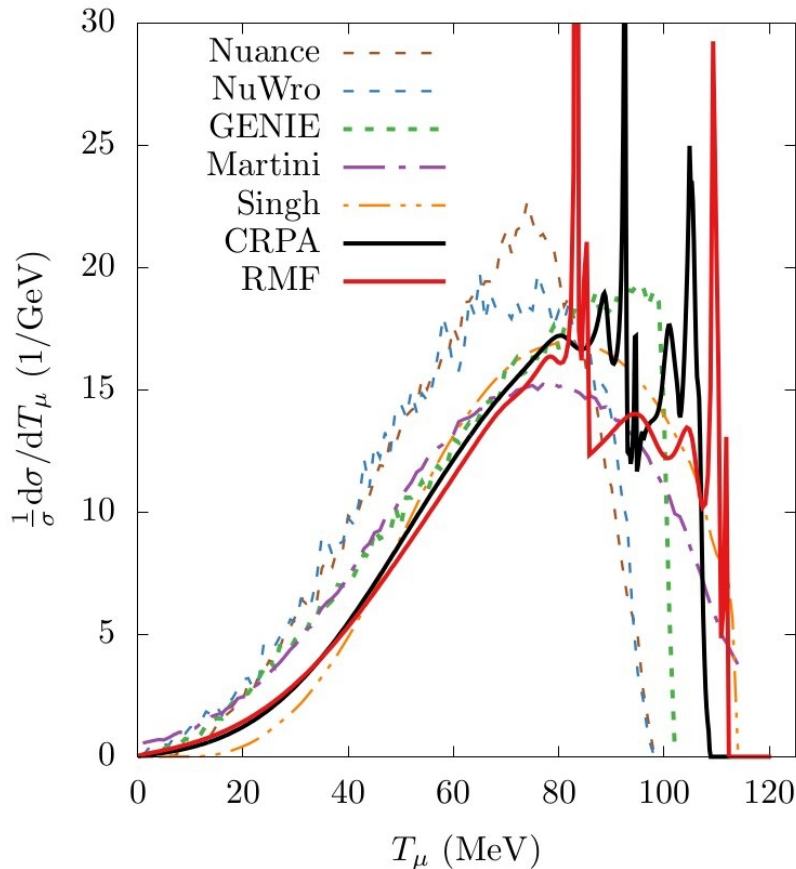


Model	$\Delta\chi^2$	$\chi^2$ Prob.	$\sigma$ ( $10^{-39}\text{cm}^2$ )
Nuance	2.64	0.45	1.4
NuWro	2.07	0.56	$1.3 + 0.4$ (np-nh)
GENIE	0.95	0.81	1.75
Martini	2.15	0.54	$1.3 + 0.2$ (np-nh)
Singh	3.90	0.27	0.91
CRPA	3.20	0.36	1.58
RMF	3.49	0.27	1.56
RFG	1.69	0.64	1.66
RFG34	4.16	0.25	1.38
MB data	-		$2.7 \pm 1.2$

$\chi^2$  basically driven by endpoint

Shape-only comparisons of different models

# MiniBooNE comparison: Model comparisons & Total cross sections



Shape-only comparisons of different models

Model	$\Delta\chi^2$	$\chi^2$ Prob.	$\sigma$ ( $10^{-39} \text{cm}^2$ )
Nuance	2.64	0.45	1.4
NuWro	2.07	0.56	$1.3 + 0.4$ (np-nh)
GENIE	0.95	0.81	1.75
Martini	2.15	0.54	$1.3 + 0.2$ (np-nh)
Singh	3.90	0.27	0.91
CRPA	3.20	0.36	1.58
RMF	3.49	0.27	1.56
RFG	1.69	0.64	1.66
RFG34	4.16	0.25	1.38
MB data	-	-	$2.7 \pm 1.2$

## Total cross sections

Most  $\sim 1.5 - 1.7$   $10^{-39} \text{cm}^2/\text{N}$

RFG34 & NUANCE  $\sim 1.4$   $10^{-39} \text{cm}^2/\text{N}$

Singh  $\sim 0.91$   $10^{-39} \text{cm}^2/\text{N}$

see also [Prog.Part.Nucl.Phys. 129 (2023) 104019]

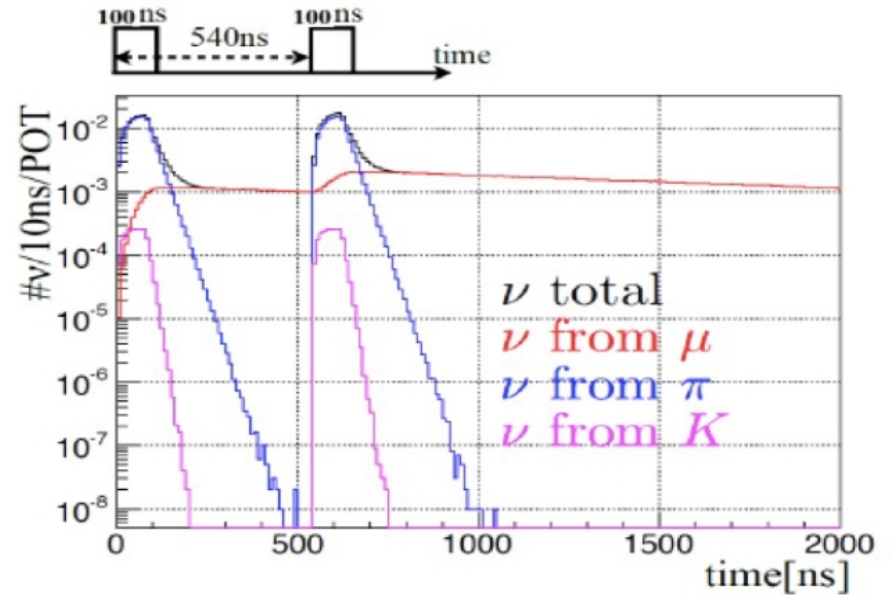
# JSNS<sup>2</sup> measurement on carbon (from Hyoungku Jeon talk NuFACT22)

Measure the total visible energy:

$$E_{\text{vis}} = E_{\nu} - m_{\mu} - T_X$$

Invisible energy  
e.g. neutrons

Sensitive to specific decay channel  
of nucleus



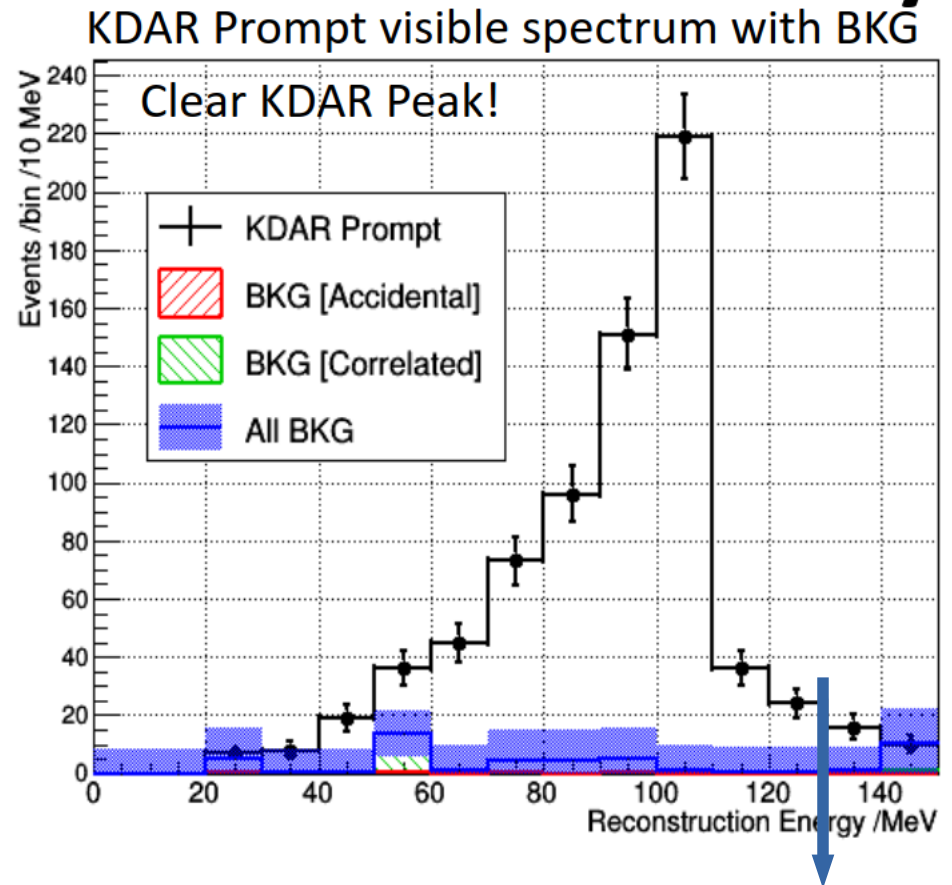
- The time distribution of neutrinos from pion, muon and kaon decays.
- the neutrino from kaon is concentrated at the proton beam bunch timing.

# JSNS<sup>2</sup> measurement (from Hyoungku Jeon talk NuFACT22)

Measure the total visible energy:

$$E_{\text{vis}} = E_{\nu} - m_{\mu} - T_{\text{X}}$$

Sensitive to specific decay channel  
of nucleus

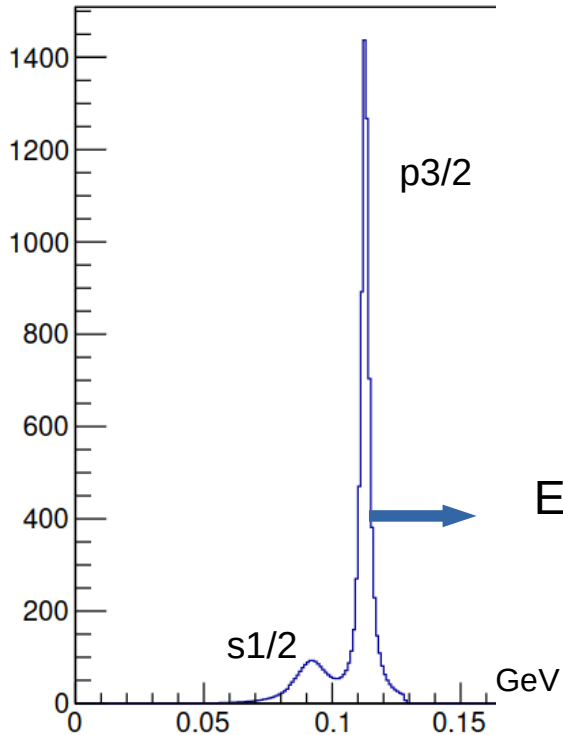


$$E_{\text{vis}}^{\text{max}} = E_{\nu} - m_{\mu}$$



# JSNS<sup>2</sup> measurement

Missing energy spectrum ( $\nu, \mu, p$ )

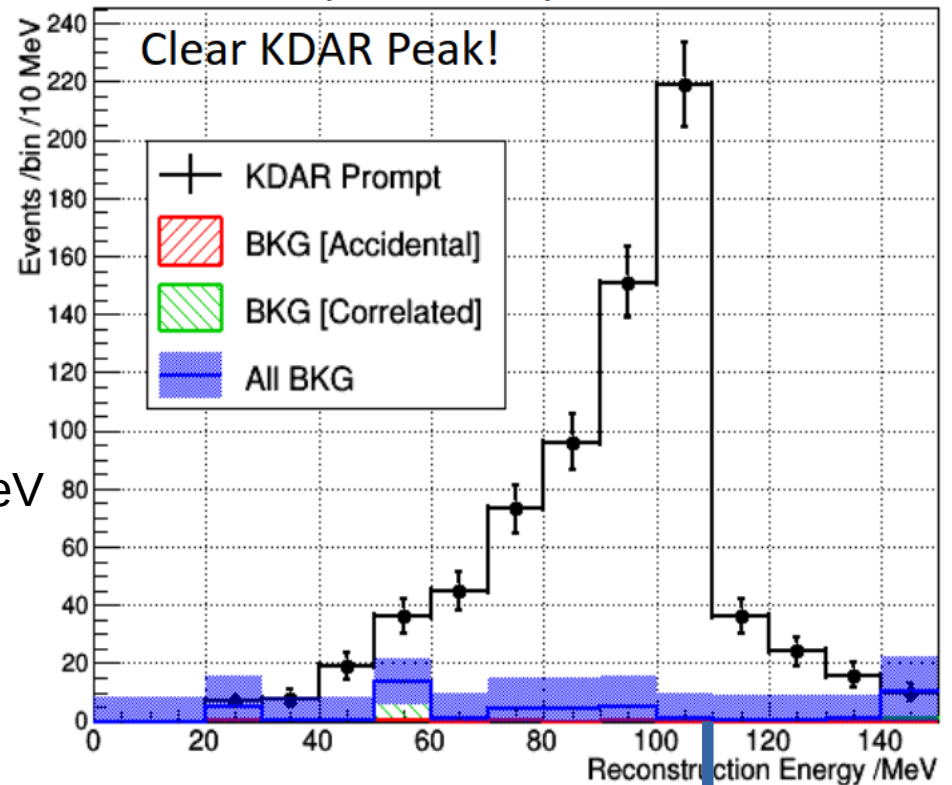


$E_s \approx 16$  MeV

RMF calculation exclusive (no FSI)  
w Benhar spectral function

Clear smearing of spectrum in data  
Need good final-state approach

KDAR Prompt visible spectrum with BKG



$$E_\nu - m_\mu - E_s$$

## Conclusions

- KDAR  $\nu_\mu$  provide charged-current signal with  $E_\nu = 236$   
→ muon kinematics as a 'clean' observable
- Muon angle dependence carries information on responses and separates low- energy excitations from 'QE'-region
- Large body of electron scattering information in the KDAR phase space  
→ Combined data constraints from e and  $\nu$  probe axial current
- HF-CRPA calculations provide robust results for different nuclei in this kinematic region  
→ Exact treatment of the continuum provides smooth behaviour over regimes
- KDAR measurements of MiniBooNE: inclusive energy spectrum
- KDAR measurements of JSNS<sup>2</sup>: missing energy distribution  
→ Requires control over 'FSI' and deexcitations  
→ Where does the FSI picture change ?